

## Article

# Parameters Identification of the Fractional-Order Permanent Magnet Synchronous Motor Models Using Chaotic Ensemble Particle Swarm Optimizer

Dalia Yousri <sup>1</sup>, Magdy B. Eteiba <sup>1</sup>, Ahmed F. Zobaa <sup>2,\*</sup> and Dalia Allam <sup>1</sup>

<sup>1</sup> Electrical Engineering Department, Faculty of Engineering, Fayoum University, Fayoum 63514, Egypt; day01@fayoum.edu.eg (D.Y.); meteiba@gmail.com (M.B.E.); drengdaliaallam@gmail.com (D.A.)

<sup>2</sup> College of Engineering, Design & Physical Sciences, Brunel University London, Uxbridge UB8 3PH, UK

\* Correspondence: azobaa@ieee.org

**Abstract:** In this paper, novel variants for the Ensemble Particle Swarm Optimizer (EPSO) are proposed where ten chaos maps are merged to enhance the EPSO's performance by adaptively tuning its main parameters. The proposed Chaotic Ensemble Particle Swarm Optimizer variants (C.EPSO) are examined with complex nonlinear systems concerning equal order and variable-order fractional models of Permanent Magnet Synchronous Motor (PMSM). The proposed variants' results are compared to that of its original version to recommend the most suitable variant for this non-linear optimization problem. A comparison between the introduced variants and the previously published algorithms proves the developed technique's efficiency for further validation. The results emerge that the Chaotic Ensemble Particle Swarm variants with the Gauss/mouse map is the most proper variant for estimating the parameters of equal order and variable-order fractional PMSM models, as it achieves better accuracy, higher consistency, and faster convergence speed, it may lead to controlling the motor's unwanted chaotic performance and protect it from ravage.

**Keywords:** chaos maps; Ensemble Particle Swarm Optimizer; Permanent Magnet Synchronous Motor



**Citation:** Yousri, D.; Eteiba, M.B.; Zobaa, A.F.; Allam, D. Parameters Identification of the Fractional-Order Permanent Magnet Synchronous Motor Models Using Chaotic Ensemble Particle Swarm Optimizer. *Appl. Sci.* **2021**, *11*, 1325. <https://doi.org/10.3390/app11031325>

Academic Editor: Javier Poza

Received: 4 January 2021

Accepted: 28 January 2021

Published: 2 February 2021

**Publisher's Note:** MDPI stays neutral with regard to jurisdictional claims in published maps and institutional affiliations.



**Copyright:** © 2021 by the authors. Licensee MDPI, Basel, Switzerland. This article is an open access article distributed under the terms and conditions of the Creative Commons Attribution (CC BY) license (<https://creativecommons.org/licenses/by/4.0/>).

## 1. Introduction

Permanent Magnet Synchronous Motor (PMSM) is one of the preferable motors due to its high efficiency, low cost, and simple structure [1]. However, PMSM performance may be disturbed considerably due to its chaotic behavior due to the disturbance of load, or the system parameters change [2,3]. This behavior is an important problem in the operation of PMSM because of torque inconstancy, low-frequency fluctuations in current, and speed oscillations, which may lead, in turn, to motor collapse. The whole system stability, safety as well as the economic operation of the industrial process may be influenced by this unwanted behavior [4]. Therefore, there is a persistent need for efficient and accurate modeling of the motor's dynamic behavior to improve the chaotic performance control and prevent the ravage of the motor [2,3]. Moreover, it is crucial to introduce an accurate and simple optimization technique to efficiently extract the parameters of these models with minimum execution time to restore the system's normal operation as soon as possible and prevent its damage [5].

Recently, fractional modeling becomes a new avenue in dynamic modeling. The fractional-order models provide a proper emulation of the system's physical response by adding new degrees of freedom for the mathematical model of the systems [6–8]. Two types of the fractional modeling of PMSM defined as an equal order and variable-order fractional models are currently published and validated to introduce more flexible and accurate modeling over the integer one [2,9]. Therefore, they are selected to be tested in this work.

In literature, two approaches are introduced to define the parameters of PMSM irregular behavior. The first one is the numerical methods that have been proposed for

determining the PMSM model's parameters at a specific operating condition [2,9]. The numerical techniques employed some simplifications and assumptions while handling such a nonlinear problem. Thus, the second approach has been proposed to identify the models' parameters using the meta-heuristic optimization techniques [10,11]. Yousri et al. [12] proposed two novel meta-heuristic optimization algorithms named Chaotic Grasshopper Optimizer (CGOA) and Chaotic Grey wolf optimizer (CGWO) in addition to their basic versions (GWO and GOA) for parameters estimation of both equal and variable-order fractional models. Nevertheless, seeking better accuracy and lower time consumption, which are significant factors in predicting and controlling the motor's unpredictable performance as fast as possible, reliable developed algorithms should be proposed for optimal parameters estimation.

The Particle Swarm Optimization Algorithm (PSO) is considered as the simplest one to be implemented and it has performed well on several fields [13]. While, there are some disadvantages in the PSO technique such as trapping in the local minimum where its searchability is insufficient and its convergence speed is slow because each particle is learned from both of the personal best as well as the global best [14]. To minimize these drawbacks, several variants of PSO have been reported in the literature to compromise between the exploration and exploitation processes. One of these variants is the Self-organizing Hierarchical PSO (HPSO-TVAC) that has been developed to reinforce the global exploration in addition to the local exploitation and thereby avoiding earlier convergence as well as reaching the global optimum during the latter stages of the search [15]. another variant known as Comprehensive Learning PSO (CLPSO) has been proposed where each particle learns from the best experiences of the other particles over various dimensions [16]. Additionally, a variant named Fitness Distance Ratio based PSO (FDR-PSO) has been introduced to enhance the capability of the local search [17]. Moreover, the variant named Distance-based locally informed PSO (LIPS) has been employed to enhance searching for multiple local optima in multi-modal problems [18]. Lately, Ensemble Particle Swarm Optimizer EPSO [19] has been proposed to combine all features of PSO, CLPSO, HPSO-TVAC, and LIPS variants in only one variant to offer robust performance in various optimization problems with different features. It is worth mentioning that the EPSO variant has an effective performance in nonlinear complicated systems. While the free lunch theorem (NFL) states that no optimizer is perfect to be employed as the best method for any optimization problem at hand [20]. Hence, any algorithm may fail to converge and provide unexpected performance as a result of the impact of some control parameters on the exploration as well as the exploitation phases. Accordingly, the behavior of the algorithm may be changed according to the variations of these parameters. Therefore, several attempts are still performed aiming to achieve a compromise between the diversification and intensification during the search process of the algorithm to provide an appropriate behavior especially in the case of non-linear optimization problem [21–25].

Lately, merging the dynamic behavior of the chaos maps and the met-heuristic algorithms has affirmed its efficiency in improving the consistency and accuracy of the standard algorithms [26,27]. In that approach, the uniform or Gaussian distributions are replaced by chaos maps in the original algorithm to use their statistical and dynamical properties in adjusting control parameters of the basic versions of the algorithms. The Chaotic Grasshopper Optimizer [12,28], Chaotic Flower pollination algorithm (CFPA) in [29], Chaotic Differential Evolutionary algorithm [30], Chaotic Whale Optimization Algorithm (CWOA) [31] and Chaotic Salp Optimizer [26] are some examples for that approach. The proposed chaotic variants of the GOA, FPA, GWO, and SSA algorithms have shown their efficiency in various optimization problems.

Therefore, In this manuscript, ten chaos maps are merged with EPSO to propose novel variants named chaotic Ensemble Particle Swarm optimizer (C.EPSO) to boost the EPSO performance while solving the non-linear optimization problem of PMSM modeling. Firstly, to validate the results of C.EPSO variants, they are compared with the results of the original EPSO intensively using different statistical analysis. Furthermore, an excessive

comparison is established between the results of the novel variants and that of the previous techniques listed in literature. The comparison clarifies that C.EPSO proves its superiority in accuracy, consistency, higher convergence rate and lower execution time. The final recommendation is C.EPSO with Gauss/mouse map is the proper variant to estimate the parameters of equal and variable order fractional models.

The manuscript is arranged as follows: Section 2 shows the fractional models of the PMSM motor. The optimization problem is mathematically modeled in Section 3. Section 4 presents the main equations of basic EPSO algorithm, the chaos maps functions and the proposed chaotic variants of EPSO. Simulation and results are emerged in Section 5. Section 6 summaries the conclusion.

## 2. Fractional PMSM Model

PMSM model has been mathematically formulated as a system of non linear differential equations. The fractional calculus is a new trend that is used to provide a better emulation of the motor physical performance and to increase the model flexibility. Thereby, the PMSM can be modeled mathematically as fractional differential equations with derivative orders lower or greater than 1 [2,9]. In this work, two fractional PMSM models are introduced. The first one is the variable order fractional model [2], while the other one is the equal order fractional model [9]. The general system of differential equations of PMSM is described as in a system of equations (Equation (1)) [2].

$$\begin{aligned}\frac{d^{q_1} i_d}{dt} &= -i_d + \omega i_q + u_d, \\ \frac{d^{q_2} i_q}{dt} &= -i_d - \omega i_q + \gamma \omega + u_q, \\ \frac{d^{q_3} \omega}{dt} &= \sigma(i_q - \omega) - T_L\end{aligned}\quad (1)$$

where  $q_i$  ( $i = 1,2,3$ ) are the fractional derivatives, the  $i_q$  and  $i_d$  and  $\omega$  are the state variables, which represent currents and motor angular frequency. The  $u_q$  and  $u_d$  are the quadrature and direct-axis stator voltage component [9,32]. The  $\gamma$  and  $\sigma$  are the system dimensionless operating parameters. The load torque is  $T_L$ .

When the inputs of the system are 0 where  $T_L = u_d = u_q = 0$ , the equations of the system in 1 is reformulated as follows in the system of equations (Equation (2)) [2].

$$\begin{aligned}\frac{d^{q_1} i_d}{dt} &= -i_d + \omega i_q, \\ \frac{d^{q_2} i_q}{dt} &= -i_d - \omega i_q + \gamma \omega, \\ \frac{d^{q_3} \omega}{dt} &= \sigma(i_q - \omega)\end{aligned}\quad (2)$$

The PMSM behaves chaotically when the equal order fractional model parameters  $\gamma$  and  $\sigma$  have values equal to 100, 10 respectively and  $q_1 = q_2 = q_3 = 0.95$  as reported in Ref. [9]. While, for the variable order fractional model, the parameters  $\gamma$ ,  $\sigma$ ,  $q_1$ ,  $q_2$  and  $q_3$  is equal to 50, 4, 0.99, 1 and 0.98, respectively as in Ref. [2]. The initial conditions at the chaotic region for equal and variable order fractional models are  $[i_d, i_q, \omega] = [2.5, 3, 1]$ .

## 3. Problem Formulation

Practically, the parameters of equal and variable order fractional models are unknown. Accurate estimation of these parameters is a problem of optimization which targets minimization of the gap between the original system and the estimated one. Therefore, developing new optimization variants to estimate the global unknown parameters optimally is a very crucial issue.

The general fractional derivative differential equation of the PMSM are described as follows (3).

$$D_t^q X(t) = f(X_t, X_0, \theta) \tag{3}$$

where  $D_t = \frac{d}{dt}$  is the time derivative operator  $t$ , the original system state vector is  $X = (i_d, i_q, \omega)^T \in R^n$  while its initial state vector is  $X_0$  and  $\theta = (\theta_1, \theta_2, \dots, \theta_d)^T = (\sigma, \gamma)^T$  is the original parameters and  $q = (q_1, q_2, q_3, \dots, q_n)^T \in R^n$  is fractional order derivatives.

While, fractional derivative differential equation with identified parameters is (4)

$$D_t^{\hat{q}} \hat{X}(t) = f(\hat{X}_t, X_0, \hat{\theta}) \tag{4}$$

where  $\hat{X} = (\hat{i}_d, \hat{i}_q, \hat{\omega})^T$  is the estimation of the state vector,  $\hat{\theta} = (\hat{\sigma}, \hat{\gamma})^T$  the vector of the extracted parameters and  $\hat{q} = (\hat{q}_1, \hat{q}_2, \hat{q}_3, \dots, \hat{q}_n)^T$  is the estimated non-integer derivative orders.

The objective function named Mean Square Error (MSE) is employed between original and identified state vectors as in Equation (5). The block diagram describing the process of the fractional model parameters estimation is emerged in Figure 1.

$$MSE = \frac{1}{k} \sum_{i=1}^k |X(i) - \hat{X}(i)|^2 \tag{5}$$

where samples number is indicated by k.

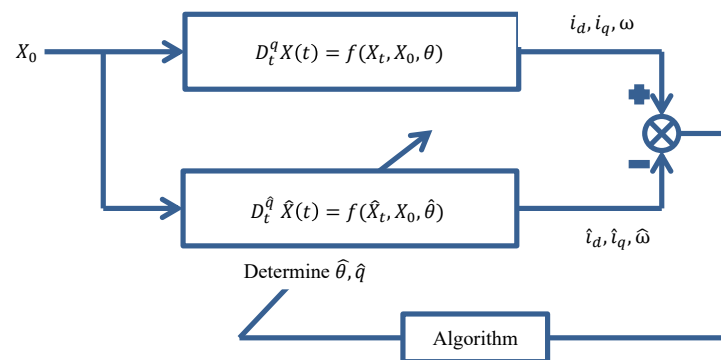


Figure 1. The block diagram for estimating the parameters of PMSM fractional models.

The core problem associated with the conventional optimization algorithms that may prevent them to converge to the global optimal parameters is occurred due to the local optima. Therefore, there is a persistent need to develop and test novel optimization techniques in this work to handle such these intricate non linear problems.

#### 4. Chaotic Ensemble Particle Swarm Optimizer (C.EPSO)

In this section, the details of the proposed algorithm for PMSM models parameters estimation process are presented.

##### 4.1. Ensemble Particle Swarm Optimizer (EPSO)

EPSO is the most recent variant of PSO that combine different variants of PSO such as CLPSO, inertia weight PSO, LIPS, HPSO-TVAC and FDR-PSO variants to create more robust algorithm that is able to solve various optimization problems of different applications [19]. The population size in EPSO is consisting of two groups of subpopulations, a small group and a large one. The small group utilizes CLPSO algorithm while the large one uses the other predetermined variants. In the large group, for updating a particle, one of PSO strategies is adaptively selected depending on the ratio of success of every methodology in

the latest iterations [19]. Mathematical control equation of PSO variants that employed in EPSO are listed as follows:

Control equations of inertia weight PSO

basic PSO is combined with a control parameter named inertia weight  $w$  to compromise between the local as well as the global searches.  $w$  has value decreased linearly with time. The velocity of a particle is computed as follows

$$V_i^d = w * V_i^d + c_1 * rand1_i^d * (pbest_i^d - Z_i^d) + c_2 * rand2_i^d * (gbest^d - Z_i^d) \quad (6)$$

where  $i$  indicates the agents ( $i = 1, 2, \dots, N$ ) while  $d$  indicates the dimension ( $d = 1, 2, \dots, D$ ).  $Z_i^d$  is the location of  $i^{th}$  particle and  $V_i^d$  is the agent velocity in the population.  $pbest_i^d$  is the best location of the particle  $i$  at  $d$  dimension. The  $gbest^d$  is the best location found by population of the swarm so far. The  $w$  is decreasing linearly in range of 0.9–0.2 during the run time [19] to enhance the balance between the global and local search.  $c_1$  and  $c_2$  are the acceleration coefficients varied with time, where  $c_1 = 2$  and  $c_2 = 2$ .  $rand1_i^d$  and  $rand2_i^d$  are random numbers in range of  $[0, 1]$ .

Control equations of modified CLPSO

CLPSO has been proposed for tackling the problem of trapping the original PSO in the local minimum and far from the global one for multi-model optimization problem [16]. In CLPSO, each particle has been learned from pbests of other particles at different dimensions. The new velocity employed in EPSO variant is as follows [16]:

$$V_i^d = w * V_i^d + c_1 * rand1_i^d * (pbest_{f_i(d)}^d - Z_i^d) + c_2 * rand2_i^d * (gbest^d - Z_i^d) \quad (7)$$

where  $pbest_{f_i(d)}^d$  is the best place of a particle  $i$ ,  $f_i(d) = [f_i(1), f_i(2), \dots, f_i(D)]$  shows that  $i^{th}$  particle moves to its own or to the other's  $pbest_i^d$  for each dimension  $d$ .  $c_1$  and  $c_2$  are time varying acceleration coefficients,  $c_1$  is used in the range of 2.5–0.5 while  $c_2$  is used in the range of 0.5–2.5.  $rand1_i^d$  and  $rand2_i^d$  are randomly generated numbers in the range of  $[0, 1]$ .

Control equations of FDR-PSO

FDR-PSO has been introduced to address the convergence problem in PSO. In FDR-PSO, each particle learns from the neighboring particle's experience ( $nbest$ ) that have a better fitness than itself. Consequently, the  $i^{th}$  particle's velocity component in  $d^{th}$  dimension is upgraded through the following equation [17]:

$$V_i^d = w * V_i^d + c_1 * rand1_i^d * (pbest_i^d - Z_i^d) + c_2 * rand2_i^d * (gbest^d - Z_i^d) + c_3 * (nbest_i^d - Z_i^d) \quad (8)$$

where  $c_1$ ,  $c_2$  and  $c_3$  are time varying acceleration coefficients, they equal to 1, 1 and 2, respectively.  $nbest$  is the experience of neighboring particle.

Control equations of HPSO-TVAC

HPSO-TVAC has been introduced to avoid premature convergence in the early stages and enhance the convergence to the global optimum solution [15]. In HPSO-TVAC technique, the particle's velocity is updated as follows [15]:

$$V_i^d = c_1 * rand1_i^d * (pbest_i^d - Z_i^d) + c_2 * rand2_i^d * (gbest^d - Z_i^d) \quad (9)$$

where  $c_1$  and  $c_2$  are time varying acceleration coefficients,  $c_1$  is used in the range of 2.5–0.5 while  $c_2$  is used in the range of 0.5–2.5.

Control equations of LIPS

In LIPS, neighboring particles' best experiences is utilized for particles' guidance instead of the best experience of the swarm. The velocity of the particle is as follows:

$$V_i^d = \chi * (V_i^d + \varphi(P_i^d - Z_i^d)),$$

where

$$P_i^d = \frac{\sum_{j=1}^{nsize} (\varphi_j * nbest_j) / nsize}{\varphi}, \tag{10}$$

$$\varphi_j \sim U\left(0, \frac{4.1}{nsize}\right), \quad \varphi = \sum_{j=1}^{nsize} \varphi_j$$

where,  $nbest_j$  is defined as the nearest neighborhood of  $j^{th}$  particle to  $pbest$  of  $i$  particle.  $nsize$  is the neighborhood size that is dynamically increased  $n$  range of [2, 5]. The constriction coefficient  $\chi$  is equal to 0.7298. The  $\varphi_j$  is a positive number drawn randomly from a uniform distribution in range of [0, 4.1/nize]. The acceleration weight  $\varphi$  is equal the summation of  $\varphi_j$ .

#### 4.2. Chaotic Maps

The randomization process in all the natural inspired optimization techniques is performed using Gaussian distribution. lately, a novel avenue has been created to improve this process by replacing Gaussian distribution by chaotic maps to avail from their randomization properties. In this approach, merging the features of chaos maps with the original algorithms achieves rapid convergence to the optimal solution with better accuracy especially in case of difficult problems such as multi-modal functions [33]. In this work, ten different one-dimensional chaos maps are utilized to adjust some control parameters of the basic version of EPSO algorithm and subsequently achieving a better convergence rate and more accurate results. The novel chaotic variants are named Chaotic Ensemble Particle Swarm Optimizer (C-EPSO). The utilized chaos maps are listed in Table 1. The distribution values is equal to the maximum number of iterations and the initial value is equal to 0.7.

**Table 1.** Chaotic maps formulas [33].

Number	Function Name	Chaotic Map
1	Chebyshev	$x_{i+1} = \cos(i \cos^{-1}(x_i))$
2	Circle	$x_{i+1} = \text{mod}(x_i + b - (\frac{a}{2\pi}) \sin(2\pi x_k, 1)),$ $a = 0.5$ and $b = 0.2$
3	Gauss/mouse	$x_{i+1} = \begin{cases} 1 & x_i = 0 \\ \frac{1}{\text{mod}(x_i, 1)} & \text{Otherwise} \end{cases}$
4	Iterative	$x_{i+1} = \sin\left(\frac{a\pi}{x_i}\right), a = 0.7$
5	Logistic	$x_{i+1} = ax_i(1 - x_i), a = 4$
6	Piecewise	$x_{i+1} = \begin{cases} \frac{x_i}{P} & 0 \leq x_i < P \\ \frac{x_i - P}{0.5 - P} & P \leq x_i < 0.5 \\ \frac{1 - P - x_i}{0.5 - P} & 0.5 \leq x_i < 1 - P \\ \frac{1 - x_i}{P} & 1 - P \leq x_i < 1 \end{cases}, P = 0.4$
7	Sine	$x_{i+1} = \frac{a}{4} \sin(\pi x_i), a = 4$
8	Singer	$x_{i+1} = \mu(7.86x_i - 23.31x_i^2 + 28.75x_i^3 - 13.302875x_i^4),$ $\mu = 1.07$
9	Sinusoidal	$x_{i+1} = ax_i^2 \sin(\pi x_i), a = 2.3$
10	Tent	$x_{i+1} = \begin{cases} \frac{x_i}{0.7} & x_i < 0.7 \\ \frac{10}{3}(1 - x_i) & x_i \geq 0.7 \end{cases}$

where  $(x_{i+1})$  refers to the map distributions over the number of iterations  $i$ .



#### 4.3. Chaotic Ensemble Particle Swarm Optimizer (C.EPSO)

In Equations (6)–(9) in the standard version of EPSO, there are different controlled variables selected randomly and they are dominant factors that affect the performance of the EPSO algorithm. In Equations (6)–(8), the key factor is  $w$  that has large impact on EPSO convergence and its value is varied in range of [0.99, 0.2]. Moreover,  $c_1$  and  $c_2$  coefficients are essential factors that are used in the range of 2.5–0.5 and 0.5–2.5, respectively as in Equations (7) and (9). In this paper, these variables can be adaptively tuned chaotically in the same interval as described as follows:

In C.EPSO,  $w$  is decreased chaotically beginning from 0.99 until reaching to 0.2 proportional to the iterations based on Equation (11). In addition,  $c_1$ ,  $c_2$  time varying acceleration coefficients are fluctuated chaotically in range of [2.5, 0.5] and [0.5, 2.5] respectively depending on Equations (12) and (13), respectively.

$$(C - w)_k = \left( w_I - t \times \frac{(w_F - w_I)}{T} \right) + NormChaos_k; \quad (11)$$

$$(C - c_1)_k = \left( c_{1I} - t \times \frac{(c_{1F} - c_{1I})}{T} \right) + NormChaos_k; \quad (12)$$

$$(C - c_2)_k = \left( c_{2I} - t \times \frac{(c_{2F} - c_{2I})}{T} \right) + NormChaos_k; \quad (13)$$

where

$$NormChaos_k = \frac{(Chaos_k - \min(Chaos_k)) \times (b - a)}{(\max(Chaos_k) - \min(Chaos_k))} + a \quad (14)$$

where  $(C - w)_i$  is the chaotic inertia weight at  $k$  indexed chaos map.  $w_I, w_F$  are the initial value of the inertia weight as well as its final value.  $w_I$  and  $w_F$  are tuned as 0.99 and 0.2 respectively.  $(C - c_1)_k$  and  $(C - c_2)_k$  are the coefficients of Chaotic acceleration at  $k$  indexed chaos map, respectively. The initial and final ranges of  $c_1$  and  $c_2$  are in ranges of [2.5, 0.5] and [0.5, 2.5] respectively.  $NormChaos_k$  is  $k$  indexed normalization of chaos map. The  $[\min(Chaos_k), \max(Chaos_k)]$  are minimum and maximum intervals of the distribution.  $Chaos_k$  is  $k$  indexed chosen chaos map where  $k = 1, 2, 3, \dots, 10$ . while  $a, b$  are the normalization initial range and the normalization final range, respectively. The current iteration is  $t$  while the maximum number of iterations is  $T$ .

## 5. Simulation and Results

In this part, the proposed algorithms EPSO and C.EPSO are employed for estimation of fractional PMSM models' parameters. An excessive comparisons among the chaotic variants of these algorithms and the basic ones is held based on different statistical analysis. For more validation for the performance of the algorithms, another comparison is accomplished among the novel variants and the state-of-the-art algorithms.

### 5.1. Equal Order-Fractional PMSM Model

The data of equal order fractional PMSM Model is obtained from [9] where the PMSM system 2 behaves chaotically at parameters values  $\sigma, \gamma$  of 10, 100 respectively and the equal order fractional parameters  $q_1 = q_2 = q_3$  of value 0.95 as well as the initial values of  $[i_d, i_q, \omega]$  are [2.5, 3, 1]. The number of samples in the sampling vector are 100 with a step of 0.001 s.

The introduced algorithms EPSO and C.EPSO are employed to identify the parameters at which the motor behaves chaotically at 200 iteration and population size of 20. While the minimum and maximum limits of variables are within range of [5, 15] for  $\sigma$ , [80, 120] for  $\gamma$  and [0.9, 1] for all  $q$ .

The obtained results by C.EPSO and EPSO variants are listed in Table 2. The table data shows that the effect of adding chaos maps into EPSO is significant on both of their accuracy and consistency. Where, EPSO provides  $mean \pm STD$  of MSE equaled

to  $1.963 \times 10^{-16} \pm 4.601 \times 10^{-16}$  While C.EPSO offers values in range of  $10^{-26} \pm 10^{-28}$  magnitude of orders especially with Gauss/mouse and tent maps.

**Table 2.** *mean ± STD* of the extracted parameters for commensurate fractional order PMSM Model and corresponding fitness function by proposed algorithms.

Algorithms	$\sigma$ <i>mean±STD</i>	$\gamma$ <i>mean±STD</i>	$q$ <i>mean±STD</i>	<i>MSE</i> <sub>best,mean±STD</sub>	
EPSO	$10.00 \pm 1.317 \times 10^{-9}$	$100.00 \pm 9.621 \times 10^{-9}$	$0.950 \pm 5.968 \times 10^{-12}$	$3.859 \times 10^{-20}, 1.963 \times 10^{-16} \pm 5.242 \times 10^{-16}$	
C.EPSO	C.EPSO1	$10.00 \pm 2.777 \times 10^{-15}$	$100.00 \pm 1.498 \times 10^{-14}$	$0.950 \pm 0.00$	$4.416 \times 10^{-26}, 4.511 \times 10^{-26} \pm 8.140 \times 10^{-28}$
	C.EPSO2	$10.00 \pm 1.872 \times 10^{-15}$	$100.00 \pm 9.474 \times 10^{-15}$	$0.950 \pm 0.00$	$4.416 \times 10^{-26}, 4.436 \times 10^{-26} \pm 5.016 \times 10^{-28}$
	C.EPSO3	$10.00 \pm 1.776 \times 10^{-15}$	$100.00 \pm 9.474 \times 10^{-15}$	<b><math>0.950 \pm 0.00</math></b>	$4.416 \times 10^{-26}, 4.432 \times 10^{-26} \pm 4.985 \times 10^{-28}$
	C.EPSO4	$10.00 \pm 2.512 \times 10^{-15}$	$100.00 \pm 1.340 \times 10^{-14}$	$0.950 \pm 0.00$	$4.416 \times 10^{-26}, 4.448 \times 10^{-26} \pm 6.646 \times 10^{-28}$
	C.EPSO5	$10.00 \pm 3.077 \times 10^{-15}$	$100.00 \pm 1.641 \times 10^{-14}$	$0.950 \pm 0.00$	$4.416 \times 10^{-26}, 4.464 \times 10^{-26} \pm 7.614 \times 10^{-28}$
	C.EPSO6	$10.00 \pm 2.512 \times 10^{-15}$	$100.00 \pm 1.340 \times 10^{-14}$	$0.950 \pm 0.00$	$4.416 \times 10^{-26}, 4.448 \times 10^{-26} \pm 6.646 \times 10^{-28}$
	C.EPSO7	$10.00 \pm 2.512 \times 10^{-15}$	$100.00 \pm 1.340 \times 10^{-14}$	$0.950 \pm 0.00$	$4.416 \times 10^{-26}, 4.448 \times 10^{-26} \pm 6.646 \times 10^{-28}$
	C.EPSO8	$10.00 \pm 3.077 \times 10^{-15}$	$100.00 \pm 1.641 \times 10^{-14}$	$0.950 \pm 0.00$	$4.416 \times 10^{-26}, 4.464 \times 10^{-26} \pm 7.614 \times 10^{-28}$
	C.EPSO9	$10.00 \pm 2.512 \times 10^{-15}$	$100.00 \pm 1.340 \times 10^{-14}$	$0.950 \pm 0.00$	$4.416 \times 10^{-26}, 4.448 \times 10^{-26} \pm 6.646 \times 10^{-28}$
	C.EPSO10	$10.00 \pm 2.777 \times 10^{-15}$	$100.00 \pm 1.641 \times 10^{-14}$	<b><math>0.950 \pm 0.00</math></b>	$4.416 \times 10^{-26}, 4.468 \times 10^{-26} \pm 7.438 \times 10^{-28}$
	$10.00 \pm 1.776 \times 10^{-15}$	$100.00 \pm 9.474 \times 10^{-15}$		$4.416 \times 10^{-26}, 4.432 \times 10^{-26} \pm 4.985 \times 10^{-28}$	

As the time factor and the algorithm convergence speed are essential factors, the mean convergence curves are plotted in Figure 2 to emerge the swiftness of convergence rate of the C.EPSO over the basic version. Where C.EPSO variants reach to lower MSE values compared to EPSO at 80 iteration however EPSO required more iterations trying to reach for closer values to that of C.EPSO as shown in the zoomed figure on Figure 2. Regarding for the execution time of the proposed algorithms are 4.951118 and 5.5194925 s for the C.EPSO and EPSO algorithms, respectively.

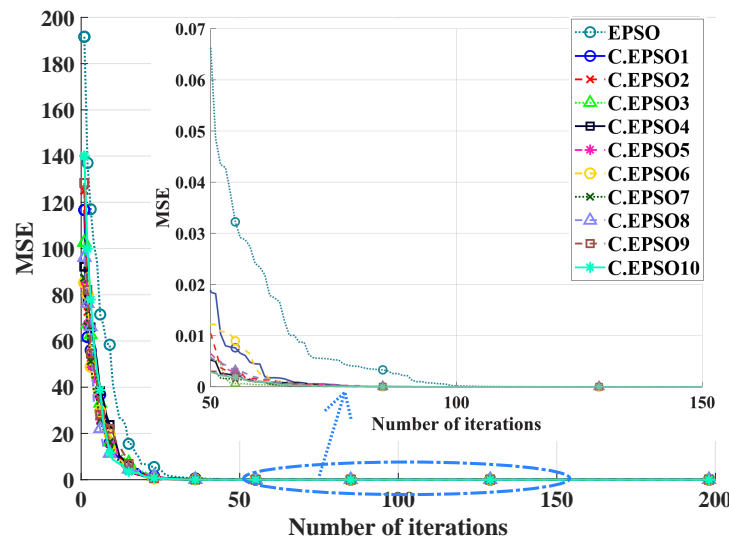


**Figure 2.** Average convergence curves by C.EPSO variants versus the standard EPSO for the commensurate fractional order PMSM model of ten chaos maps.

Based on the previous results, it's obvious that merging chaos maps especially the Gauss/mouse and tent maps with the EPSO improves its accuracy, consistency of the results and convergence speed considerably. As C.EPSO with Gauss/mouse and tent maps provide *mean ± STD* values of MSE equal to  $4.432 \times 10^{-26}$  and  $4.985 \times 10^{-28}$ , respectively. Furthermore, the convergence curves indicate that the C.EPSO variants reach to the minimum values of MSE with lower number of iterations and execution time.

### 5.2. Variable Order Fractional PMSM Model

In this section, EPSO and novel C.EPSO variants are utilized to estimate parameters of variable order fractional model using data in [2]. Where the PMSM system 2 behaves



chaotically at values of parameters  $\gamma, \sigma, q_1, q_2$  and  $q_3$  equal to 50, 4, 0.99, 1 and 0.98 respectively as well as initial values of  $[i_d, i_q, \omega]$  equal to [2.5, 3, 1]. The number of samples is 100 in the sampling vector with a step equal to 0.001 s.

The number of iterations is 500, the number of search agents are 50 while the minimum and maximum limits of variables are in range of [2, 8] for  $\sigma$ , [40, 60] for  $\gamma$  and [0.9, 1] for all  $q_s$ . A comparison is accomplished among the results of all variants over 20 independent runs to determine the most efficient one.

The identified parameters' Mean values and STD as well as the cost function's value are tabulated in Table 3. Table 3 indicates that consolidating chaotic maps with the basic algorithms has a sensible impact on the accuracy as well as the homogeneity of the results. Where, the *mean*  $\pm$  *STD* of MSE resulted by EPSO have been improved in the range of  $10^{-10} \pm 10^{-12}$  when C.EPSO version is used especially with Sine map.

The mean convergence curves over 20 independent runs in Figure 3 illustrate that the convergence speed of EPSO has been improved as a result of the combination of chaos maps with the basic technique. Where, the C.EPSO decaying rate of convergence is faster than EPSO especially with Gauss/mouse map additionally C.EPSO variants started to converge nearly at 140 iteration while EPSO consumes larger number of iterations. For execution time of the C.EPSO and EPSO, the total run time are equaled to 56.9135 and 58.2056 ,respectively.

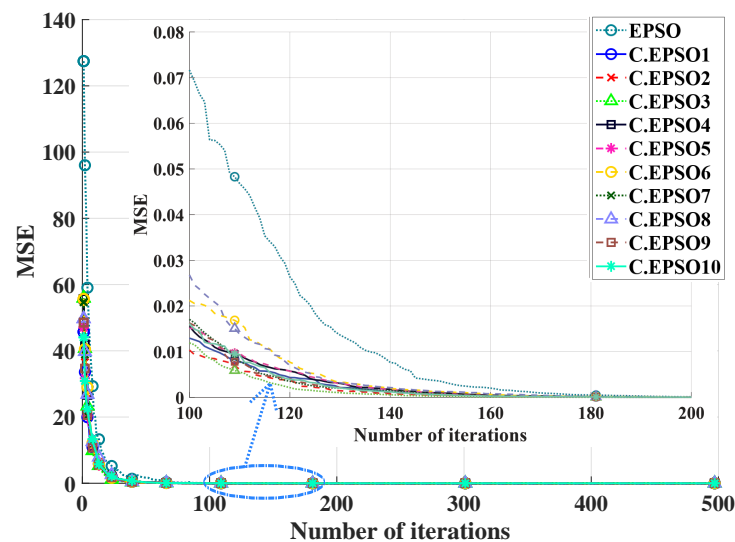


**Figure 3.** Average convergence curves by the C.EPSO and standard algorithms EPSO for the incommensurate fractional order PMSM model of ten chaos maps.

To summarize the overall result, it is obvious that chaos maps have a preferable effect on the performance of EPSO from the points of accuracy, consistency and convergence speed to the optimal solutions. C.EPSO offers more consistent results especially C.EPSO7. From the convergence curves, C.EPSO outperforms EPSO with shorter execution time especially C.EPSO3.

**Table 3.** *mean ± STD* of the extracted parameters for incommensurate fractional order PMSM Model and corresponding fitness function by proposed algorithms.

Algorithms		$\sigma$ <i>mean±STD</i>	$\gamma$ <i>mean±STD</i>	$q_1$ <i>mean±STD</i>	$q_2$ <i>mean±STD</i>	$q_3$ <i>mean±STD</i>	<i>MSE</i> <i>best,mean±STD</i>
	EPSO	$4.00 \pm 1.023 \times 10^{-9}$	$50.00 \pm 3.730 \times 10^{-9}$	$0.990 \pm 1.429 \times 10^{-10}$	$1.00 \pm 2.872 \times 10^{-10}$	$0.980 \pm 3.080 \times 10^{-10}$	$6.466 \times 10^{-20}, 2.473 \times 10^{-16} \pm 9.326 \times 10^{-16}$
C.EPSO	C.EPSO1	$4.00 \pm 7.593 \times 10^{-15}$	$50.00 \pm 4.890 \times 10^{-15}$	$0.990 \pm 6.753 \times 10^{-16}$	$1.00 \pm 5.919 \times 10^{-16}$	$0.980 \pm 7.751 \times 10^{-16}$	$1.385 \times 10^{-27}, 3.916 \times 10^{-27} \pm 5.076 \times 10^{-27}$
	C.EPSO2	$4.00 \pm 5.563 \times 10^{-15}$	$50.00 \pm 5.877 \times 10^{-15}$	$0.990 \pm 6.223 \times 10^{-16}$	$1.00 \pm 3.350 \times 10^{-16}$	$0.980 \pm 5.842 \times 10^{-16}$	$1.385 \times 10^{-27}, 2.383 \times 10^{-27} \pm 1.508 \times 10^{-27}$
	C.EPSO3	$4.00 \pm 6.153 \times 10^{-15}$	$50.00 \pm 3.993 \times 10^{-15}$	$0.990 \pm 5.758 \times 10^{-16}$	$1.00 \pm 4.549 \times 10^{-16}$	$0.980 \pm 6.739 \times 10^{-16}$	$1.385 \times 10^{-27}, 2.847 \times 10^{-27} \pm 2.630 \times 10^{-27}$
	C.EPSO4	$4.00 \pm 6.016 \times 10^{-15}$	$50.00 \pm 5.877 \times 10^{-15}$	$0.990 \pm 6.929 \times 10^{-16}$	$1.00 \pm 3.761 \times 10^{-16}$	$0.980 \pm 6.656 \times 10^{-16}$	$1.385 \times 10^{-27}, 2.965 \times 10^{-27} \pm 1.995 \times 10^{-27}$
	C.EPSO5	$4.00 \pm 3.583 \times 10^{-15}$	$50.00 \pm 3.993 \times 10^{-15}$	$0.990 \pm 5.913 \times 10^{-16}$	$1.00 \pm 2.483 \times 10^{-16}$	$0.980 \pm 3.752 \times 10^{-16}$	$1.385 \times 10^{-27}, 2.259 \times 10^{-27} \pm 7.593 \times 10^{-28}$
	C.EPSO6	$4.00 \pm 4.245 \times 10^{-15}$	$50.00 \pm 3.260 \times 10^{-15}$	$0.990 \pm 4.899 \times 10^{-16}$	$1.00 \pm 2.671 \times 10^{-16}$	$0.980 \pm 4.945 \times 10^{-16}$	$1.385 \times 10^{-27}, 2.186 \times 10^{-27} \pm 1.354 \times 10^{-27}$
	C.EPSO7	$4.00 \pm 5.357 \times 10^{-15}$	$50.00 \pm 7.290 \times 10^{-15}$	$0.990 \pm 6.108 \times 10^{-16}$	$1.00 \pm 9.865 \times 10^{-17}$	$0.980 \pm 3.483 \times 10^{-16}$	$1.385 \times 10^{-27}, 2.120 \times 10^{-27} \pm 5.423 \times 10^{-28}$
	C.EPSO8	$4.00 \pm 5.657 \times 10^{-15}$	$50.00 \pm 6.313 \times 10^{-15}$	$0.990 \pm 5.962 \times 10^{-16}$	$1.00 \pm 1.709 \times 10^{-16}$	$0.980 \pm 3.812 \times 10^{-16}$	$1.385 \times 10^{-27}, 2.103 \times 10^{-27} \pm 7.127 \times 10^{-28}$
	C.EPSO9	$4.00 \pm 6.471 \times 10^{-15}$	$50.00 \pm 5.155 \times 10^{-15}$	$0.990 \pm 5.990 \times 10^{-16}$	$1.00 \pm 5.201 \times 10^{-16}$	$0.980 \pm 6.428 \times 10^{-16}$	$1.385 \times 10^{-27}, 2.912 \times 10^{-27} \pm 3.123 \times 10^{-27}$
	C.EPSO10	$4.00 \pm 4.080 \times 10^{-15}$	$50.00 \pm 2.823 \times 10^{-15}$	$0.990 \pm 5.516 \times 10^{-16}$	$1.00 \pm 3.311 \times 10^{-16}$	$0.980 \pm 5.288 \times 10^{-16}$	$1.385 \times 10^{-27}, 2.537 \times 10^{-27} \pm 1.609 \times 10^{-27}$

### 5.3. Comparison with the Latest Published Algorithms in Literature

GOA, GWO algorithms and their chaos variants are the only published meta-heuristic optimization algorithms for estimating equal and variable order fractional PMSM models as in [12]. The authors in [12] modified GOA and GWO for improving both of the accuracy and the rapidity of convergence of the basic algorithms. In this subsection, an excessive comparison is accomplished among the results of the novel variants and that of the literature algorithms GOA, GWO and their chaotic variants.

Based on the results in [12], the best variants in CGWO and CGOA in case of equal order fractional model are CGWO1 and CGOA5. These variants achieved  $2.7590 \times 10^{-7}$ ,  $\pm 8.7827 \times 10^{-6}$  and  $1.7935 \times 10^{-14}$ ,  $\pm 8.5292 \times 10^{-6}$ , respectively. While, C.EPSO, the C.EPSO3 and C.EPSO10 offer *best*,  $\pm STD$  values of *MSE* equal to  $4.432 \times 10^{-26} \pm 4.985 \times 10^{-28}$ , respectively. These results prove that the newly developed variants provide more authenticity and consistency of the results than CGWO and CGOA best variants which subsequently affects on the veracity of identifying the corresponded parameters for the chaotic behavior in motor.

In case of variable order fractional model, C.EPSO3 and C.EPSO7 exhibits *best* values of *MSE* equal to  $1.385 \times 10^{-27}$  with *STD* values are  $2.630 \times 10^{-27}$  and  $5.423 \times 10^{-28}$ , respectively. However, the best variants of CGWO and CGOA are CGWO7 and CGOA2 have achieved  $3.9396 \times 10^{-6}$ ,  $\pm 1.6357 \times 10^{-4}$  and  $2.4653 \times 10^{-10}$ ,  $\pm 6.7161 \times 10^{-2}$ , respectively. By this way, the current work introduces more efficient technique than that in literature as C.EPSO variants achieve more veracity and uniformity of results.

Additionally, the convergence curves of the best variants of the proposed algorithm (C.EPSO) and that of the previously published ones (CGWO and CGOA) are plotted in Figure 4 for the two fractional models. Figure 4a is indicating the case of equal order fractional model where C.EPSO3 and C.EPSO10 show the lower mean values of *MSE* with faster convergence speed compared with CGWO1 and CGOA5. Likewise, for variable order fractional model as in Figure 4b, C.EPSO3 and C.EPSO7 exhibit the lower mean values of *MSE* with faster speed of convergence. Accordingly, the (C.EPSO3, C.EPSO10) and (C.EPSO3, C.EPSO7) achieve the most optimal and consistent solutions with the fastest convergence speed for both of equal and variable order fractional models compared to the other algorithms.

The main outcome is that by introducing the C.EPSO, the optimal parameters at which the motor behaves chaotically are identified accurately and that will affect in turn on improving of the accuracy of the control process of the motor chaos and ensure the protection of motor from ravage as well.

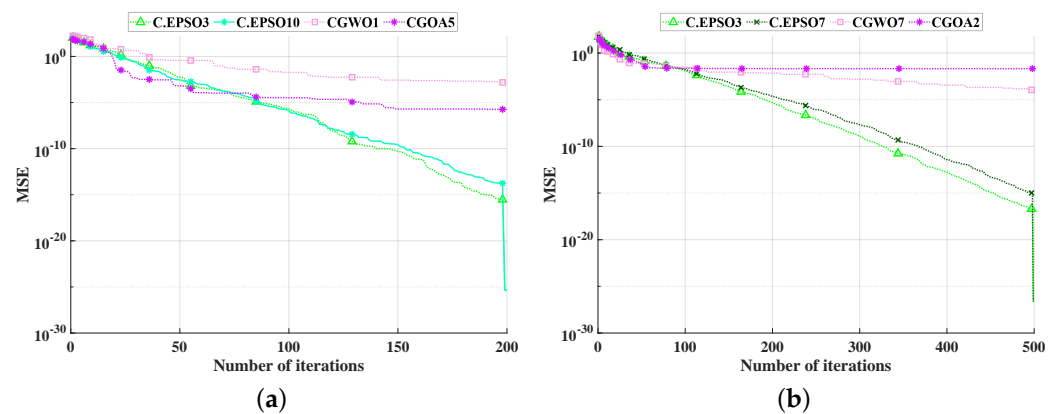


**Figure 4.** Average convergence curves by the best chaotic variants of the proposed algorithms (C.EPSO, EPSO) and comparable ones (CGWOA, CGOA) for (a) C-FO-M, and (b) InC-FO-M .

## 6. Conclusions

Equal order and variable-order fractional PMSM models have currently introduced to increase the motor modeling's accuracy and flexibility. These models have enhanced the motor's physical depiction despite their complexity in parameter identification. Therefore, this work's main target is achieving a proper parameters estimation for these complicated fractional models to control motor behavior in the chaotic region. Lately, meta-heuristic algorithms are considered a powerful tool for identifying these intricate problems. Improving such algorithms using novel avenues as chaos maps to modify their characteristics has been regarded as a recent trend. The latest PSO variant named EPSO is proposed and developed by combining ten chaos maps to improve its accuracy and efficiency. As a result, the Chaotic Ensemble Particle Swarm Optimizer variants (C.EPSO) have been proposed. The novel variants' results were compared to that of the standard version of EPSO and that of the published algorithms using an intensive statistical analysis. The results have shown that the C.EPSO with Gauss/mouse map is the most recommended variant for identifying the parameters of equal order and variable-order fractional PMSM models, respectively. It has given less error, high convergence speed, and short execution time. This variant has achieved an accurate and rapid prediction of the parameters at which the motor chaos behavior. Subsequently, this may lead to a quick control of the motor and better protection from ravage.

**Author Contributions:** All the authors have the same contribution. All authors have read and agreed to the published version of the manuscript.

**Funding:** This research received no external funding.

**Institutional Review Board Statement:** Not applicable.

**Informed Consent Statement:** Not applicable.

**Data Availability Statement:** The data are available on request from the corresponding author.

**Conflicts of Interest:** The authors declare no conflict of interest.

## References

1. Dambrauskas, K.; Vanagas, J.; Zimnickas, T.; Kalvaitis, A.; Ažubalis, M. A Method for Efficiency Determination of Permanent Magnet Synchronous Motor. *Energies* **2020**, *13*, 1004. [[CrossRef](#)]
2. Li, C.L.; Yu, S.M.; Luo, X.S. Fractional-order permanent magnet synchronous motor and its adaptive chaotic control. *Chin. Phys. B* **2012**, *21*, 100506. [[CrossRef](#)]
3. Li, C.L.; Wu, L. Optik Sliding mode control for synchronization of fractional permanent magnet synchronous motors with finite time. *Opt. Int. J. Light Electron Opt.* **2016**, *127*, 3329–3332. [[CrossRef](#)]
4. Luo, S.; Gao, R. Chaos control of the permanent magnet synchronous motor with time-varying delay by using adaptive sliding mode control based on DSC. *J. Frankl. Inst.* **2018**, *355*, 4147–4163. [[CrossRef](#)]
5. Yu, J.; Chen, B.; Yu, H.; Gao, J. Nonlinear Analysis: Real World Applications Adaptive fuzzy tracking control for the chaotic permanent magnet synchronous motor drive system via backstepping. *Nonlinear Anal. Real World Appl.* **2011**, *12*, 671–681. [[CrossRef](#)]
6. Rajagopal, K.; Vaidhyanathan, S.; Karthikeyan, A.; Duraisamy, P. Dynamic analysis and chaos suppression in a fractional order brushless DC motor. *Electr. Eng.* **2016**. [[CrossRef](#)]
7. Gu, W.; Yu, Y.; Hu, W. Parameter estimation of unknown fractional-order memristor-based chaotic systems by a hybrid artificial bee colony algorithm combined with differential evolution. *Nonlinear Dyn.* **2016**, *84*, 779–795. [[CrossRef](#)]
8. Cruz-Duarte, J.M.; Rosales-García, J.; Correa-Cely, C.R.; Garcia-Perez, A.; Avina-Cervantes, J.G. A closed form expression for the Gaussian-based Caputo-Fabrizio fractional derivative for signal processing applications. *Commun. Nonlinear Sci. Numer. Simul.* **2018**, *61*, 138–148. [[CrossRef](#)]
9. Xue, W.; Li, Y.; Cang, S.; Jia, H.; Wang, Z.; Xue, W.; Li, Y.; Cang, S.; Jia, H.; Wang, Z. Chaotic behavior and circuit implementation of a fractional-order permanent magnet synchronous motor model. *J. Frankl. Inst.* **2015**, *352*, 2887–2898. [[CrossRef](#)]
10. Biswas, P.P.; Suganthan, P.N.; Amaratunga, G.A.J. Optimization of Wind Turbine Rotor Diameters and Hub Heights in a Windfarm Using Differential Evolution Algorithm. In *Advances in Intelligent Systems and Computing*; Springer: Singapore, 2017; pp. 131–141. [[CrossRef](#)]
11. Qu, B.Y.; Liang, J.J.; Zhu, Y.S.; Suganthan, P.N. Solving dynamic economic emission dispatch problem considering wind power by multi-objective differential evolution with ensemble of selection method. *Nat. Comput.* **2017**. [[CrossRef](#)]

12. Yousri, D.; Allam, D.; Eteiba, M. Parameters Identification of Fractional Order Permanent Magnet Synchronous Motor Models Using Chaotic Meta-Heuristic Algorithms. In *Mathematical Techniques of Fractional Order Systems*; Elsevier: Amsterdam, The Netherlands, 2018; pp. 529–558.
13. Yuan, L.; Yang, Q. Parameter identification of fractional-order chaotic systems without or with noise: Reply to comments. *Commun. Nonlinear Sci. Numer. Simul.* **2018**. [[CrossRef](#)]
14. Lynn, N.; Suganthan, P.N. Heterogeneous comprehensive learning particle swarm optimization with enhanced exploration and exploitation. *Swarm Evol. Comput.* **2015**, *24*, 11–24. [[CrossRef](#)]
15. Ratnaweera, A.; Halgamuge, S.; Watson, H. Self-Organizing Hierarchical Particle Swarm Optimizer With Time-Varying Acceleration Coefficients. *IEEE Trans. Evol. Comput.* **2004**, *8*, 240–255. [[CrossRef](#)]
16. Liang, J.; Qin, A.; Suganthan, P.; Baskar, S. Comprehensive learning particle swarm optimizer for global optimization of multimodal functions. *IEEE Trans. Evol. Comput.* **2006**, *10*, 281–295. [[CrossRef](#)]
17. Peram, T.; Veeramachaneni, K.; Mohan, C.K. Fitness-distance-ratio based particle swarm optimization. In Proceedings of the Swarm Intelligence Symposium, SIS'03, Indianapolis, IN, USA, 26 April 2003; pp. 174–181.
18. Qu, B.Y.; Suganthan, P.N.; Das, S. A distance-based locally informed particle swarm model for multimodal optimization. *IEEE Trans. Evol. Comput.* **2013**, *17*, 387–402. [[CrossRef](#)]
19. Lynn, N.; Suganthan, P.N. Ensemble particle swarm optimizer. *Appl. Soft Comput.* **2017**, *55*, 533–548. [[CrossRef](#)]
20. Wolpert, D.H.; Macready, W.G. No free lunch theorems for optimization. *IEEE Trans. Evol. Comput.* **1997**, *1*, 67–82. [[CrossRef](#)]
21. Aljarah, I.; Mafarja, M.; Heidari, A.A.; Faris, H.; Zhang, Y.; Mirjalili, S. Asynchronous accelerating multi-leader salp chains for feature selection. *Appl. Soft Comput.* **2018**, *71*, 964–979. [[CrossRef](#)]
22. Mafarja, M.; Aljarah, I.; Heidari, A.A.; Hammouri, A.I.; Faris, H.; Al-Zoubi, A.M.; Mirjalili, S. Evolutionary Population Dynamics and Grasshopper Optimization approaches for feature selection problems. *Knowl. Based Syst.* **2018**, *145*, 25–45. [[CrossRef](#)]
23. Mafarja, M.; Aljarah, I.; Heidari, A.A.; Faris, H.; Fournier-Viger, P.; Li, X.; Mirjalili, S. Binary dragonfly optimization for feature selection using time-varying transfer functions. *Knowl. Based Syst.* **2018**, *161*, 185–204. [[CrossRef](#)]
24. Alyasseri, Z.A.A.; Khader, A.T.; Al-Betar, M.A.; Awadallah, M.A.; Yang, X.S. Variants of the flower pollination algorithm: A review. In *Nature-Inspired Algorithms and Applied Optimization*; Springer: Berlin/Heidelberg, Germany, 2018; pp. 91–118.
25. Zhang, X.; Kang, Q.; Cheng, J.; Wang, X. A novel hybrid algorithm based on Biogeography-Based Optimization and Grey Wolf Optimizer. *Appl. Soft Comput.* **2018**, *67*, 197–214. [[CrossRef](#)]
26. Sayed, G.I.; Khoriba, G.; Haggag, M.H. A novel chaotic salp swarm algorithm for global optimization and feature selection. *Appl. Intell.* **2018**, *48*, 3462–3481. [[CrossRef](#)]
27. Rizk-Allah, R.M.; Hassaniien, A.E.; Bhattacharyya, S. Chaotic crow search algorithm for fractional optimization problems. *Appl. Soft Comput.* **2018**, *71*, 1161–1175. [[CrossRef](#)]
28. Arora, S.; Anand, P. Chaotic grasshopper optimization algorithm for global optimization. *Neural Comput. Appl.* **2018**, *71*, 4385–4405. [[CrossRef](#)]
29. Yousri, D.; AbdelAty, A.M.; Said, L.A.; Elwakil, A.; Maundy, B.; Radwan, A.G. Chaotic Flower Pollination and Grey Wolf Algorithms for parameter extraction of bio-impedance models. *Appl. Soft Comput.* **2018**. [[CrossRef](#)]
30. Singh, N.J.; Dhillon, J.; Kothari, D. Multi-objective thermal power load dispatch using chaotic differential evolutionary algorithm and Powell's method. *Soft Comput.* **2018**, *22*, 2159–2174. [[CrossRef](#)]
31. Yousri, D.; Allam, D.; Eteiba, M. Chaotic whale optimizer variants for parameters estimation of the chaotic behavior in Permanent Magnet Synchronous Motor. *Appl. Soft Comput.* **2019**, *74*, 479–503. [[CrossRef](#)]
32. Li, Z.; Park, J.B.; Joo, Y.H.; Zhang, B.; Chen, G. Bifurcations and chaos in a permanent-magnet synchronous motor. *IEEE Trans. Circuits Syst. I Fundam. Theory Appl.* **2002**, *49*, 383–387. [[CrossRef](#)]
33. Mirjalili, S.; Gandomi, A.H. Chaotic Gravitational Constants for The Gravitational Search Algorithm. *Appl. Soft Comput.* **2017**, *53*, 407–419. [[CrossRef](#)]